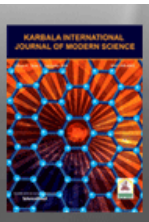

Karbala International Journal of Modern Science

Volume 6 | Issue 4 Article 6

The Deleterious F109S Mutation Disrupts Binding of Sex-Determining Region Y with DNA

Mohammed Baqur S. Al-Shuhaib MBSA
Al-Qasim Green University, baquralhilly_79@yahoo.com

The Deleterious F109S Mutation Disrupts Binding of Sex-Determining Region Y with DNA

Abstract

Sex-determining region Y (SRY) protein is the master switch in the initiation of male sex differentiation. Mutation in *SRY* gene results in ambiguous genitalia and abnormalities in reproductive organs. Its function is mainly controlled by its high mobility group (HMG) box. Damage to the HMG box may cause dysfunction of the SRY protein, which may, in turn, lead to sex reversal. This study was conducted to prioritize the deleterious effects of the non-synonymous single nucleotide polymorphisms (nsSNPs) on SRY protein. A series of computational tools were applied to predict nsSNPs with the most harmful effects on protein structure, function, and stability. Molecular docking experiments were performed to identify the possible role of these nsSNPs in altering protein binding potentials with receptors. Cumulative results indicated that three nsSNPs would have highly deleterious effects, namely I90M, F109S, and Y127F. Docking analyses revealed no participation of both I90M and Y127F in modulating the binding of SRY with its receptor DNA sequences, while F109S induced a noticeable alteration in SRY by inducing a conformational change in its HMG box. In conclusion, the predictive tools showed that I90M, F109S, and Y127F are the most drastic SNPs in the SRY, signifying possible destructive consequences of these SNPs on sex development. Both I90M and Y127F undergo such harmful effects on the structure, function, and stability without being involved in modulating SRY binding with its DNA receptor sequences. This study provides a comprehensive platform for assessing the pattern of damaging effects of nsSNPs on the *SRY* gene, which may be linked with the grade of sexual dysfunction syndromes.

Keywords

HMG box, missense, prediction, sex reversal, SNP

Cover Page Footnote

Non

1. Introduction

Sex determination is primarily controlled by a dominant switch located on the Y-chromosome. This switch is represented by the *SRY* (sex-determining region Y) gene, also referred to as the sex-determining factor [1]. It has been recognized that this gene acts as the main factor in gender determination, which is expressed during the early onset of sexual development. The *SRY* gene consists of only one exon within its sequences, with an open reading frame encoding up to 204 amino acids [2]. It is widely acknowledged that SRY protein can act as a transcription factor due to the presence of a highly conserved region known as HMG (high mobility group) box. This box is made up of 60−128 amino acids, the domain of the SRY that primarily responsible for binding with DNA [3]. Most mutations causing sex reversal are located in the HMG box and may, therefore, damage the specificity of DNA binding, demonstrating the vital role played by the HMG box in SRY activity [4]. Mutations within the *SRY* gene that are reportedly confirmed to cause male-to-female sex reversal in XY individuals are the main reason for the failure of indifferent gonads development into testes [5]. Several sex-reversal genetic syndromes have been associated with mutations in the *SRY* gene, such as 46, XY female sex reversal syndrome, Turner syndrome, Wilms' tumor 1, and Swyer syndrome [6−9]. Thus, the SNPs observed in the *SRY* gene can account for susceptibility to various diseases. However, the standard experimental methods of prioritizing the most deleterious nsSNPs are time-consuming and expensive [10]. Alternatively, the recent innovations in structural biology have made it possible to develop highly accurate *in silico* tools to predict the effects of nonsynonymous single nucleotide polymorphisms (nsSNPs) with high accuracy [11]. Although other variations may create alternative protein expression [12], these effects are not easily predicted [13]. So as the best-understood effects of protein structure and activity are attributed to nsSNPs [14]. An increasing number of prediction tools are being developed to analyze the ultimate effects of each nsSNP on protein structure, function, stability, and interaction. Recent studies have begun to unravel the destructiveness of nsSNPs by providing a cumulative indication of the effects of missense variants on the analyzed proteins [15−17]. However, the *SRY* gene has not yet been comprehensively covered, and only limited state-of-the-art *in silico* tools have been employed to prioritize the effects of nsSNPs in this crucial genetic locus. Taking these data into consideration, the present study aims to provide extensive predictions of the effects of all nsSNPs on the *SRY* gene, with a particular emphasis on the mechanisms of the most harmful nsSNPs in inducing their deleterious effects on the SRY protein.

2. Materials and methods

2.1. Data sets

A total of 177 SNPs were retrieved from the NCBI-dbSNP (build 150) (https://www.ncbi.nlm.nih.gov/snp/) and ensemble browser, GRCh37 Release 101 (https://asia.ensembl.org/index.html) database of the *SRY* gene (Gene ID: 6736), including 9 in the mRNA 5′ UTR (untranslated region), 39 missense mutations or nsSNPs, 109 silent synonymous SNPs, 3 frameshift mutations, 9 stop-gain mutations, and 8 in the mRNA 3′ UTR. All of the nsSNPs were selected for further prediction analyses (Suppl. Table 1).

2.2. 3-Dimensional modeling

To predict the effects of the retrieved nsSNPs, a highly qualified, full-length 3D structure of SRY protein must be generated. The UniProtKB accession number for SRY is Q05066, and its NCBI reference sequence is NP_003131.1. A partial 3-D structure is available in online data deposited in the protein data bank, ver. 3.3 (https://www.rcsb.org/). Only a small portion of the 3-D structure for SRY is deposited under the PDB (Protein Data Bank) number 1HRZ; it covers only 74 out of the 204 amino acid residues constituting the total 3-D structure. A full-length tertiary structure of normal SRY was generated by using five different protein structure prediction servers, including Rosetta (https://robetta.bakerlab.org/) [18], Lomets (local meta-threading-server) (https://zhanglab.ccmb.med.umich.edu/LOMETS/) [19], RaptorX (http://raptorx.uchicago.edu/) [20], PhryRe2 (protein homology/analogY recognition engine) (http://www.sbg.bio.ic.ac.uk/~phyre2/html/page.cgi?id=index) [21], and I-TASSER (iterative threading assembly Refinement) (https://zhanglab.ccmb.med.umich.edu/I-TASSER/) [22]. The efficiency of each utilized tool to generate 3D structures of SRY was evaluated by qualitative

https://doi.org/10.33640/2405-609X.2082

model energy analysis (QMEAN) (https://swissmodel.expasy.org/qmean/help) [23], and side–chain parameters and Psi/Phi Ramachandran plot of PROCHECK tool (https://www.ebi.ac.uk/thornton-srv/software/PROCHECK/) [24]. Based on the comparative validations carried out for each method, the best modeler of SRY protein was chosen to act as a favorite 3D structure for further prediction analyses.

2.3. Sequence-function analysis

The possible deleterious effects of nsSNPs on protein structure and function were predicted using SIFT (Sorting Intolerant From Tolerant) (http://sift.bii.a-star.edu.sg/www/SIFT_seq_submit2.html) [25], PolyPhen (Polymorphism Phenotyping)-2 (http://genetics.bwh.harvard.edu/pph2/) [26], Panther (protein analysis through evolutionary relationships) (http://www.pantherdb.org/tools/) [27], Provean (protein variation effect analyzer) (http://provean.jcvi.org/index.php) [28], PhD-SNP (predictor of human deleterious single nucleotide polymorphisms) (http://snps.biofold.org/phd-snp/phd-snp.html) [29], SNPs&Go (predicting disease associated variations using GO terms) (https://snps-and-go.biocomp.unibo.it/snps-and-go/) [30], SNAP2 (predicting functional effect of sequence variants) (https://www.predictprotein.org) [31], P-Mut (http://mmb.irbbarcelona.org/PMut) [32], VEST (variant effect scoring) (http://hg19.cravat.us/CRAVAT/) [33], and SUSPect (disease-susceptibility-based SAV phenotype prediction) (http://www.sbg.bio.ic.ac.uk/~suspect/) [34]. The cumulative outcomes of utilized tools were assessed for each analyzed nsSNP.

2.4. Stability analysis

The stability of the mutants SRY proteins was assessed using different prediction tools, which they also based on sequences, structure, or both, including I-Mutant2 (http://folding.biofold.org/cgi-bin/i-mutant2.0) [35], CUPSAT (Cologne University Protein Stability Analysis Tool) (http://cupsat.uni-koeln.de) [36], mCSM (http://biosig.unimelb.edu.au/mcsm/) [37], SDM (http://marid.bioc.cam.ac.uk/sdm2/prediction) [38], DUET (http://biosig.unimelb.edu.au/duet/) [39], Mupro (http://mupro.proteomics.ics.uci.edu/) [40], iStable (integrated predictor for protein stability change upon single mutation) (http://predictor.nchu.edu.tw/istable/) [41], and DynaMut (http://biosig.unimelb.edu.au/dynamut/prediction) [42]. The cumulative outputs for stability prediction tools were measured and compared with structural-functional predictions. Only entirely deleterious nsSNPs were included in the further analyses.

2.5. Post-translational and evolutionary analyses

The potential effects of the most deleterious nsSNPs were assessed using AWESOME software (http://www.awesome-hust.com) [43]. Binding with ligand and receptor was predicted using a variety of protein–protein and protein-ligand prediction tools, including RaptorX [20], COACH (https://zhanglab.ccmb.med.umich.edu/COACH/) [44], TM-SITE (https://zhanglab.ccmb.med.umich.edu/TM-score/) [45], COFACTOR (https://zhanglab.ccmb.med.umich.edu/COFACTOR/) [46], FINDSITE (http://cssb.biology.gatech.edu/findsite) [47], and ConCavity (http://compbio.cs.princeton.edu/concavity/) [48]. Whereas conserved residues positioning was conducted using the ConSurf tool (http://consurf.tau.ac.il/2016/) [49].

2.6. Superimposition of SRY with its high-risk nsSNPs

A site-specific amino acid substitution was conducted by mutating the native SRY PDB file using the Swiss model PDB viewer tool ver.4.1.0 [50]. Subsequently, energy minimization for the constructed tertiary models of normal and mutants SRY was conducted to remove overhaul distorted geometries using the steepest descent energy minimization provided Gromacs parameter set [51]. The refined models of normal of SRY protein and its detected risky mutants' forms were superimposed with each other's using YASARA (Yet Another Scientific Artificial Reality Application) tool (http://yasara.org/servers.html) [52].

2.7. Docking

A suitable double-stranded DNA substrate for the binding with SRY protein was created using Chimera UCSF software ver. 1.13.1 [53]. The sequence generated for this binding was 5′-[N9]ATAACAAAT [N9]-3′, which was known to be recognized from the HMB box of SRY with the highest affinity [2]. The refined PDB formats of normal SRY, as well as its most dangerous mutant forms, were subjected to molecular docking with DNA substrate using Hex 8.0.0 tool [54]. The default procedure of docking was used, in which the maximum rotational increments for SRY receptor and DNA ligand was enabled by setting the angle to 180°. The 3D expansion parameters were set at default (N = 25 for 3D expansion and N = 18 for a steric

scan). Out of 10 clusters, only the top 2000 orientations were retained to obtain 10,000 the lowest ordered docking energy score. The docking outputs were visualized using PyMol software ver. 7.0.1 (The PyMOL Molecular Graphics System, Schrödinger, LLC.) (www.shrodinger.com).

3. Results

3.1. Model quality and structure assessment

The 3D modeling of SRY was conducted by comparing five (Rosetta, Lomets, RaptorX, PhyRe2, and I-TASSER) 3D modeling prediction tools. Validation by QMEAN scores, PROCHECK tools, and Ramachandran plot revealed a highly qualified 3D SRY generated by Rosetta (Suppl. Table 2), while the other four (Lomets, RaptorX, PhyRe2, and I-TASSER) 3D modeling tools, had given less qualified values respectively (Suppl. Fig. 1).

3.2. Structure and function prediction

A total of ten (SIFT, PolyPhen-2, PANTHER, Provean, PhD SNP, SNPs&Go, SNAP2, P-Mut, VEST, and SUSPect) different *in silico* tools were utilized.

Table 1
Cumulative predictions for the deleterious missense SNPs on SRY protein in terms of structure and function.

No.	Variant ID	mutation	SIFT	PolyPhen2	PANTHER	PROVEAN	PhD SNP	SNPs&Go	SNAP2	P-Mut	VEST	SUSPect
1.	rs1271064684	A5V	**0**[a]	**0.999**	1	−0.730	4	4	−33	0.18	0.9557	45
2.	rs104894971	S18N	0.30	0	1	−0.630	3	4	**80**	0.17	0.096	44
3.	rs1262320780	N24I	**0**	**0.843**	1	**−3.267**	**2**	2	**33**	0.42	0.659	32
4.	rs1206716616	R29W	**0.01**	**0.998**	1	−0.510	4	1	**41**	0.48	0.574	33
5.	rs1556370576	R30I	**0.01**	**0.904**	1	**−2.878**	6	2	**51**	0.33	0.629	40
6.	rs1459783583	F34L	0.76	0	1	−0.014	5	7	−8	0.23	0.981	30
7.	rs767481926	E50K	0.21	**0.945**	1	−0.245	4	4	**56**	**0.52**	0.641	20
8.	rs1223685980	S52G	0.97	0.002	1	1.076	8	9	−29	**0.52**	0.866	25
9.	rs1325077544	S52N	0.44	**0.791**	1	−0.052	4	4	−35	**0.52**	0.889	26
10.	rs762003265	Q57R	**0.04**	0.010	1	**−2.764**	**1**	3	−7	**0.55**	0.605	19
11.	rs773764555	D58E	**0.05**	0.005	1	−2.381	**1**	2	−1	0.28	0.930	24
12.	rs104894957	V60L	**0**	**0.820**	1	**−2.771**	**5**	**4**	**93**	**0.74**	0.140	**97**
13.	rs764249635	V60A	**0**	**0.997**	1	**−3.843**	**6**	**7**	**58**	**0.63**	**0.031**	**96**
14.	rs104894969	**M64I**	**0**	**0.895**	**912**	**−3.615**	**7**	**8**	**93**	**0.82**	**0.049**	**97**
15.	rs1326404572	F67Y	**0**	**0.999**	**912**	**−2.899**	**8**	**6**	**69**	**0.72**	0.080	**92**
16.	rs104894968	I68T	**0**	**0.594**	1	**−2.700**	**6**	**5**	**97**	**0.72**	0.201	**99**
17.	rs763174397	V69L	**0.03**	0.256	**912**	**−2.684**	**8**	**8**	**44**	**0.68**	0.169	**70**
18.	rs776339584	D73E	0.60	**0.973**	1	−2.087	**0**	3	**15**	**0.72**	0.708	**69**
19.	rs1057519627	R76L	**0**	**1.000**	1	−6.612	**9**	**8**	**60**	**0.78**	0.090	**89**
20.	rs770778716	R84T	**0.01**	0.000	1	−1.716	3	4	**1**	0.30	0.767	**54**
21.	rs746931713	M85K	**0**	**0.971**	1	**−5.536**	**8**	**6**	**75**	**0.78**	0.066	**96**
22.	rs1556370554	E89A	**0**	**0.876**	1	**−5.828**	**9**	**5**	**49**	**0.71**	**0.026**	**87**
23.	rs104894959	**I90M**	**0**	**0.999**	**912**	**−2.960**	**7**	**4**	**94**	**0.76**	**0.017**	**99**
24.	rs104894974	**G95R**	**0**	**1.000**	**912**	**−7.919**	**7**	**8**	**97**	**0.62**	**0.040**	**98**
25.	rs104894972	**G95E**	**0**	**1.000**	**912**	**−7.919**	**8**	**8**	**96**	**0.84**	**0.021**	**97**
26.	rs1166279862	K99N	**0**	**0.998**	1	**−4.904**	**6**	**5**	**55**	**0.68**	0.208	**78**
27.	rs104894964	K106I	**0**	**1.000**	**912**	**−7.914**	**6**	**8**	**94**	**0.84**	**0.010**	**99**
28.	rs104894956	**F109S**	**0**	**1.000**	**912**	**−7.845**	**7**	**6**	**94**	**0.84**	**0.005**	**99**
29.	rs104894966	A113T	**0**	**1.000**	1	**−3.966**	**7**	**5**	**95**	**0.82**	**0.006**	**99**
30.	rs771449441	E122K	**0.67**	**0.202**	**1**	**−0.846**	**3**	**5**	−27	**0.68**	0.812	40
31.	rs104894973	**Y127F**	**0**	**0.998**	**912**	**−3.764**	**6**	**6**	**87**	**0.76**	**0.024**	**97**
32.	rs375342012	K128R	**0.03**	**0.771**	1	**−2.800**	**8**	6	−2	**0.72**	0.265	**65**
33.	rs104894976	R133W	0	**1.000**	1	**−7.177**	**6**	**8**	**95**	**0.84**	0.129	**69**
34.	rs754623064	E156D	0.3	0.004	1	−0.956	5	6	**10**	**0.64**	0.895	25
35.	rs748958243	Y164C	**0**	0.001	1	**−5.225**	**5**	**4**	**45**	0.12	0.949	**63**
36.	rs1194771063	H182Y	1	0.399	1	0.226	8	7	**9**	0.46	0.745	30
37.	rs1019354171	P184L	0.07	0.001	1	−2.024	6	6	**52**	**0.55**	0.547	34
38.	rs780561417	N187S	0.31	0.070	1	−1.533	5	6	−1	**0.58**	0.899	19
39.	rs756606002	R197C	**0**	0.003	1	−0.807	6	6	**41**	**0.65**	0.617	19

[a] The bold numbers refer to the deleterious/damaging effect, while the non-bold letters refer to the neutral/non-damaging effect of SNPs.

Cumulative results concerned with the prediction of structural-functional consequences indicated a concordant deleterious effect for six nsSNPs, including M64I, I90M, G95R, G95E, F109S, and Y127F, on the SRY protein structure and function (Table 1).

3.3. Stability prediction

The effects of nsSNPs on protein stability were analyzed using eight computational tools, including I-Mutant2, CUPSAT, mCSM, SDM, DUET, Mupro, iStable, and DynaMut. Cumulative results predicted the effect of all the nsSNPs on protein stability and indicated concordant deleterious effects of seven nsSNPs, I68T, I90M, K99N, F109S, Y127F, E156D, and N187S (Table 2).

Both structural-functional and stability prediction analyses revealed concordant deleterious effects in three nsSNPs, namely I90M, F109S, and Y127F. Since this study was only concerned with the entirely deleterious nsSNPs, the other deleterious SNPs that did not exhibit a concordant deleterious effect were eliminated from further analyses. Out of 39 nsSNPs, three (I90M, F109S, and Y127F) damaging nsSNPs reported from all tools were described in Fig. 1. Both SNAP2 and iStable predicted the highest number of deleterious SNPs in both sets of *in silico* tools, respectively.

Table 2
Cumulative predictions for the deleterious missense SNPs on SRY protein in terms of stability.

No.	Variant ID	mutation	I-Mutant2	CUPSAT	mCSM	SDM	DUET	Mupro	iStable	DynaMut
1.	rs1271064684	A5V	**−0.42**[a]	**−1.41**	**−0.16**	0.45	0.287	0.819	0.505	1.098
2.	rs104894971	S18N	**−0.65**	**−0.61**	**−0.904**	**−0.35**	**−0.62**	**−0.429**	**0.649**	0.527
3.	rs1262320780	N24I	0.79	0.45	0.314	1.35	0.887	0.580	0.802	1.484
4.	rs1206716616	R29W	**−0.73**	**−7.46**	**−0.573**	0.24	**−0.527**	**−0.522**	**0.764**	0.055
5.	rs1556370576	R30I	**−0.37**	**−0.11**	0.374	**−0.27**	0.493	**−0.121**	**0.734**	0.354
6.	rs1459783583	F34L	**−1.52**	**0.73**	**−0.395**	**−0.2**	**−0.186**	**−0.480**	**0.777**	0.292
7.	rs767481926	E50K	**−1.45**	0.31	0.49	**−0.5**	0.5999	**−0.772**	**0.726**	0.483
8.	rs1223685980	S52G	**−2.14**	0.35	**−0.275**	0.16	0.185	**−0.819**	**0.877**	**−0.142**
9.	rs1325077544	S52N	**−0.15**	0.50	**−0.416**	0.22	0.034	**−0.008**	**0.591**	0.088
10.	rs762003265	Q57R	**−0.73**	1.56	0.205	0.34	0.552	**0.591**	**0.836**	0.88
11.	rs773764555	D58E	**−1.54**	1.03	**−0.194**	0.53	0.22	**−0.024**	**0.567**	0.587
12.	rs104894957	V60L	**−0.93**	**−1.68**	**−0.535**	**−0.66**	**−0.379**	**−1**	**0.889**	0.367
13.	rs764249635	V60A	**−2.15**	**−2.14**	**−1.193**	**−1.16**	**−1.215**	**−1**	**0.889**	0.115
14.	rs104894969	M64I	**−1.23**	**−2.5**	**−0.799**	0.61	**−0.277**	**−0.363**	**0.704**	0.079
15.	rs1326404572	F67Y	**−1.42**	0.77	0.145	0.47	0.265	**−1**	**0.852**	0.897
16.	rs104894968	**I68T**	**−2.65**	**−0.31**	**−1.452**	**−2.21**	**−1.914**	**−1**	**0.876**	**−2.309**
17.	rs763174397	V69L	**−0.38**	**−1.54**	**−0.453**	0.68	0.074	**−0.460**	**0.607**	2.07
18.	rs776339584	D73E	**−1.24**	0.61	**−0.707**	1.37	**−0.259**	**−0.163**	**0.533**	0.379
19.	rs1057519627	R76L	**−0.54**	**−0.73**	0.407	0.3	0.438	0.555	**0.693**	0.231
20.	rs770778716	R84T	**−0.85**	**−0.65**	0.122	**−0.96**	**−0.278**	**−1**	**0.861**	**−0.211**
21.	rs746931713	M85K	**−1.50**	0.98	**−0.672**	**−0.47**	**−0.625**	**−0.870**	**0.851**	**−0.149**
22.	rs1556370554	E89A	0.03	0.48	**−0.936**	**−0.1**	**−0.266**	**−0.425**	**0.520**	**−0.181**
23.	rs104894959	**I90M**	**−0.87**	**−1.03**	**−1.089**	**−0.63**	**−1.115**	**−0.820**	**0.915**	**−0.181**
24.	rs104894974	G95R	**−0.79**	**−2.04**	**−0.664**	1.24	**−0.216**	**−0.067**	**0.813**	2.001
25.	rs104894972	G95E	**−0.09**	**−0.53**	**−0.97**	1.86	0.176	**−0.277**	**0.608**	2.334
26.	rs1166279862	**K99N**	**−0.28**	**−0.1**	**−0.197**	**−0.69**	**−0.26**	**−0.398**	**0.764**	**−0.307**
27.	rs104894964	K106I	1.19	**−0.61**	0.182	0.19	0.512	0.110	0.819	0.054
28.	rs104894956	**F109S**	**−1.18**	**−1.72**	**−2.883**	**−0.53**	**−2.909**	**−0.915**	**0.848**	**−2.557**
29.	rs104894966	A113T	**−1.15**	0.53	**−1.626**	**−0.95**	**−1.656**	**−0.354**	**0.854**	0.986
30.	rs771449441	E122K	**−0.79**	**−0.16**	0.323	**−0.86**	**−0.056**	**−0.855**	**0.869**	**−0.19**
31.	rs104894973	**Y127F**	**−0.10**	**−2.33**	**−0.9**	**−0.25**	**−0.186**	**−0.570**	**0.562**	**−0.428**
32.	rs375342012	K128R	0.63	**−0.68**	**−0.121**	0.05	**−0.314**	**−0.798**	**0.705**	**−0.652**
33.	rs104894976	R133W	**−0.64**	0.92	**−0.154**	0.24	**−0.266**	**−0.741**	**0.744**	0.759
34.	rs754623064	**E156D**	**−0.54**	**−2.79**	**−0.364**	**−0.34**	**−0.751**	**−0.102**	**0.732**	**−0.864**
35.	rs748958243	Y164C	0.41	3.33	0.201	**−0.06**	0.416	**−1.266**	0.575	0.582
36.	rs1194771063	H182Y	0.94	**−1.12**	1.464	0.31	1.425	0.010	0.769	0.789
37.	rs1019354171	P184L	0.40	**−5.47**	**−0.292**	2.37	0.363	**0.263**	**0.674**	0.186
38.	rs780561417	**N187S**	**−0.63**	**−0.54**	**−0.058**	**−1.46**	**−0.013**	**−0.495**	**0.797**	**−0.411**
39.	rs756606002	R197C	**−0.80**	0.75	**−0.011**	0.05	**−0.064**	**−1**	**0.620**	0.024

[a] The bold letters refer to the deleterious/damaging effect, while the non-bold letters refer to the neutral/non-damaging effect of SNPs.

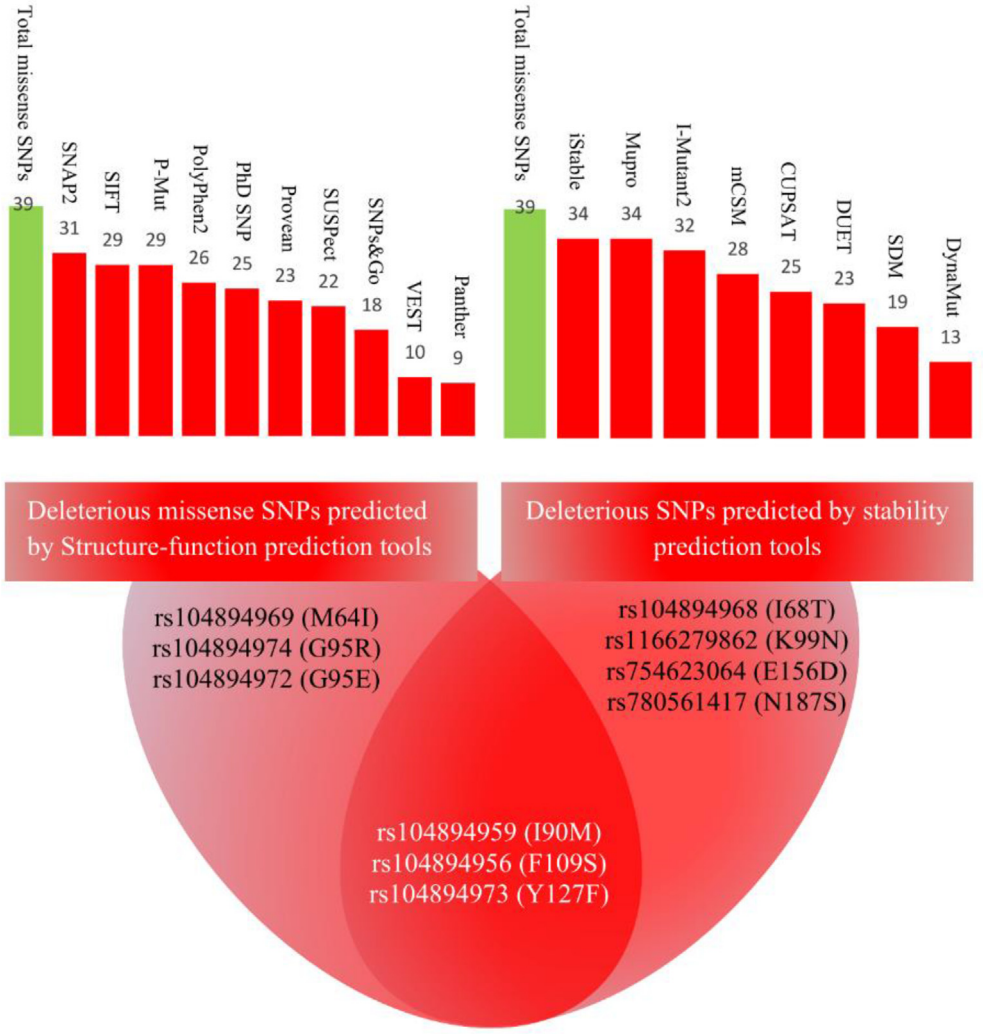

Fig. 1. The most deleterious nsSNPs of *SRY* gene as predicted by *in silico* tools in terms of structure−function and stability consequences.

3.4. Positioning analyses

Further analyses were conducted on the most three deleterious (I90M, F109S, and Y127F) nsSNPs to explore the pattern of each one in inducing such drastic alteration in the mutant SRY proteins. Analysis of ConSurf revealed highly conserved positions for both I90M and Y127F than F109S (Fig. 2, A). Meanwhile, the secondary structure prediction by UGENE indicated highly critical positions occupied by I90M and F109S. This observation was made due to the positioning of each one within a particular α-helix region (Fig. 2, B), whereas Y127F resided in a loop region held between two α-helices. However, all these three deleterious nsSNPs were positioned within the HMG (60−128) region. In the predicted 3D structure of the SRY protein, further details were provided for each nsSNP before and upon mutation (Fig. 2, C).

3.5. Post-translational modification and ligand binding prediction

The post-translational effects of the I90M, F109S, and Y127F predicted more participation of F109S in phosphorylation and O-linked β-N-acetylglucosamine dynamic protein modification. However, Y127F participated only in modulating phosphorylation, while M90I was not contributed in any of the measured post-translational activities. The possibility of the three highly risky nsSNPs to be positioned in the binding activity sites with other proteins was analyzed by utilizing seven prediction tools, namely RaptorX,

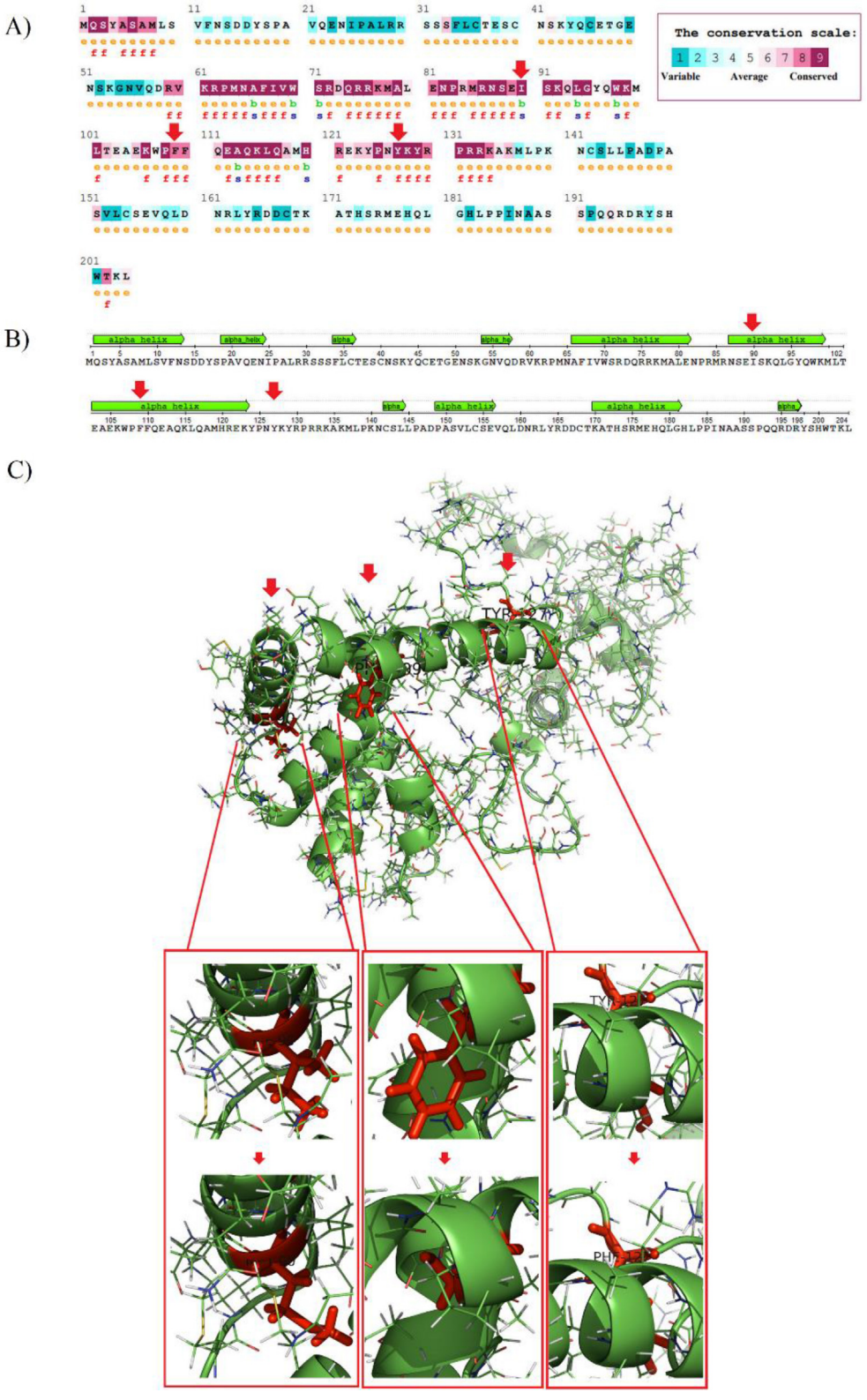

Fig. 2. Primary, secondary, and three-dimensional structure of the most harmful missense SNPs in SRY protein, namely I90M, F109S, and Y127F. Primary, secondary, and three-dimensional structures of the most harmful missense nsSNPs in SRY protein are shown in A, B, and C respectively.

COACH, TM-SITE, S-SITE, COFACTOR, FINDSITE, and ConCavity. All the utilized tools revealed no participation in any anticipated binding of the mutated amino acid residues in the 190 M, F109S, and Y127F mutant proteins with other protein receptors (Suppl. Table 3).

3.6. Superimposition prediction

Higher RMSD scores indicate a greater variation between native and mutant structures with a consequent higher effect on protein function. The superimposing of 3 mutants and wild SRY models indicated a close homology between template and targets by RMSD score of less than 0.2 Å (Fig. 3).

This observation revealed a fair superimposition of I90M, F109S, and Y127F mutant models over template SRY structure. The total energy values for the native SRY (−13909.753 kJ/mol) structure and the three mutant modeled structures I90M (−13927.618 kJ/mol), F109S (−13863.120 kJ/mol), and Y127F (−13874.935 kJ/mol) revealed 0.128%, 0.335% and 0.251% of deviation in total energy values of I90M, F109S, and Y127F respectively. Two out of three mutant modeled structures, F109S, and Y127F showed an increase in energy in comparison with the native structure. These less favourable changes indicated a more deleterious nature of both F109S and Y127F models than the I90M.

3.7. Docking with consensus DNA sequences

The molecular docking between the normal SRY and its three risky mutants was performed to identify the variation in the overall SRY-DNA interaction energy before and upon mutation. A double-stranded DNA molecule was created by introducing the SRY recognition sequences in the middle of the created DNA molecule surrounding by two flanking regions of 9 nucleic acid residues. However, the docking of this specified DNA molecule with SRY protein indicated no interaction of the I90M and Y127F in inducing any remarkable change in the binding with DNA. Meanwhile, a noticeable change in the binding energy of F109S with DNA (−627.6 kcal/mol) compared with the DNA binding energy of the wild SRY (−650.6 kcal/mol) was observed. This indicated modulation was originated from an interesting tilt in the α-helix fragment, in which the mutant 109Ser residue resided (Fig. 4).

4. Discussion

Mutations in human SRY are associated with several disorders of sex development, which may lead to sex reversal in some cases [55]. However, until recently, it is not known how the damaged SRY binds with its cognate DNA sequences [56]. Therefore, it is necessary to provide an insight into the putative mechanisms through which these mutations can cause these drastic effects on the SRY, with the possible subsequent alteration in sex development [57].

Due to the straightforward effect of nsSNPs on the protein function and activity compared with the other variations, the current study highlighted nsSNPs using a series of computational tools based on a variety of algorithms to prioritize the most dangerous amino acid substitutions on the SRY protein. The numbers of coding SNPs of the *SRY* gene were found to be higher than SNPs detected in the 5′ and 3′ untranslated regions. This is due to the nature of the sequence variations to majorly acting on the structure of gene

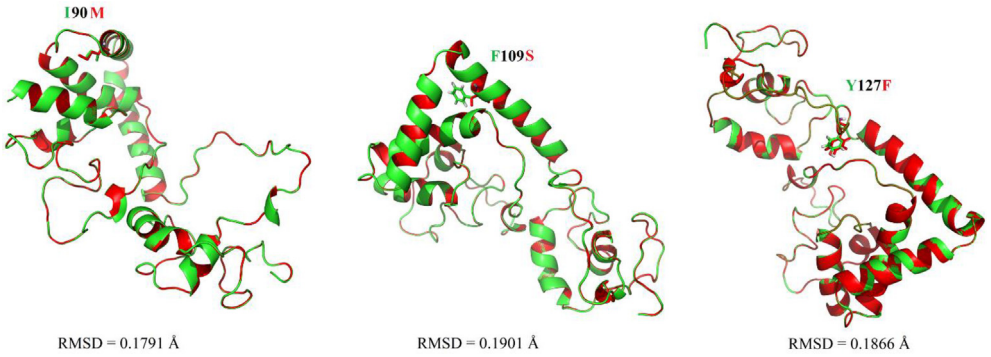

Fig. 3. Root mean square deviation (RMSD) parameters for the most deleterious nsSNPs of the *SRY* gene. Green and red colors refer to native and mutants, respectively.

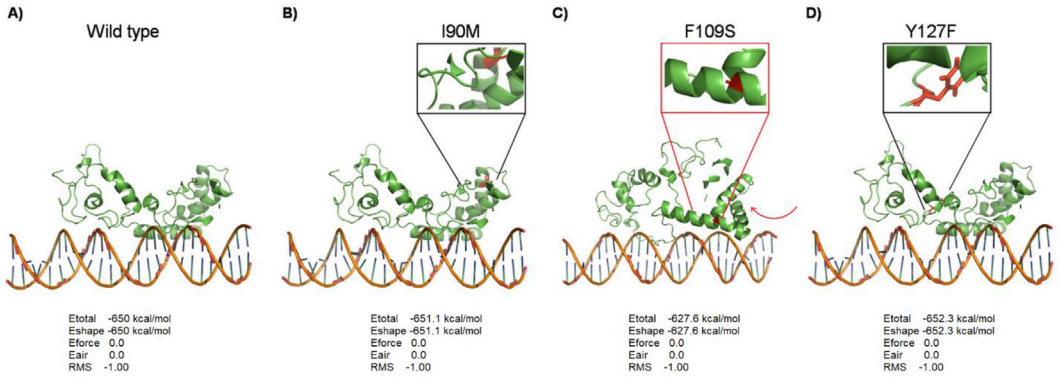

Fig. 4. Comparative docking parameters of SRY native and its mutant forms of I90M, F109S, and Y127F with DNA substrate A – D, respectively. The red curved arrow refers to the effect of F109S in altering the conformation of SRY.

products rather than on regulating the expression of the gene itself [58]. Accordingly, the retrieved nsSNPs were comprehensively highlighted in terms of their cumulative effects on structure, function, and stability.

This study observed three highly deleterious nsSNPs, I90M, F109S, and Y127F, by utilizing 26 available structure–function-stability prediction tools. The high degree of evolutionary conservation for these risky nsSNPs may justify some serious contribution of these nsSNPs to damaging SRY.

Interestingly, the three risky nsSNPs resided within the HMG domain. This domain, in turn, is being occupied within a highly evolutionary conserved region extended from 60 to 128 residues [59]. Thus, it is mandatory to investigate the role of these variations in the possible interruption of HMG activity with respect to its binding with the corresponding DNA consensus sequence 5'-[AT]AACAA [AT]-3' [2]. To understand the possible role of the observed nsSNPs in modulating this binding, molecular docking was exploited. Docking was performed by interacting 3D structures of normal SRY and its deleterious mutants with the same DNA target. Though no significant contribution of I90M and Y127F were observed in changing SRY binding with DNA, a clear change was proven in the case of F109F. This noticeable change in binding affinity with its corresponding DNA was attributed to a conformational alteration in the F109S SRY, which entails a series of undesired consequences for this alteration due to the replacement of the aromatic phenylalanine residue with a nonaromatic serine residue. As is was inferred from this study, F109S induces a remarkable bend in the SRY protein with subsequent alteration in the SRY-DNA binding conformation. This sort of deleterious substitution in SRY may unmask the multi-faceted molecular functions of this specific DNA-bending mechanism and its consequent effect on SRY- related human sex development [60,61].

In contrast to I90M and Y127F, the amino acid substitution of F109S occurred in the vicinity to the binding site with DNA which may provide a dramatic modification in the affinity of SRY-DNA interaction. This finding is supported in this study by the apparent ability of F109S to be involved in more post-translational dynamic activities than Y127F and I90M, respectively. In agreement with this finding, it is indicated that F109S substitution leads to interruption of the alpha-helical stretch that being extended from 99 to 128 amino acid residues [62]. However, it was found that the wild type SRY protein binds to its specified DNA sequence, whereas the mutant SRY carrying this amino acid substitution fails to bind, or binds with negligible activity [63,64].

Whatever the pattern nsSNPs take in the interruption of SRY activity, these three risky nsSNPs were found to be associated with several sex reversal issues [62,65,66]. However, I90M and Y127F undergo their deleterious tasks by a straightforward effect on structure, function, and stability without being intervened in the modulation of SRY binding with its DNA receptor. Meanwhile, F109S follows another mechanism, in which it rather induces a conformational change in the 3D structure of SRY to force it to alter its binding nature with DNA sequences. This amino acid substitution deserves more attention as male development is sensitive to alterations in SRY-DNA architecture [60]. Therefore, F109S is involved in the conversion of the tertiary structure of SRY in such a way it affects the subsequent binding with DNA sequences. Therefore, it can be stated that such altered binding between the mutant F109S SRY and its corresponding DNA sequences would disrupt sexual development.

5. Conclusions

This study predicted three (I90M, F109S, and Y127F) highly deleterious nsSNPs, which was revealed by all tools concerned with the prediction of structure−function, and stability. Although I90M and Y127F were not found to be contributed in modulating the binding activity of mutant SRY with its corresponding receptor DNA, F109S exhibited a noticeable reduction in this activity. This remarkable reduction signifies a more dramatic role driven by F109S substitution in altering the binding of SRY with receptor DNA. Consequently, the mechanism of the intervention of F109S in changing the conformation of the mutant SRY is revealed. This study provides in-depth interpretation for clinicians to assess the severity of sex reversal-linked syndromes by knowing the type of drastic effect of each deposited nsSNP on SRY protein.

Funding

Authors declare that this work was not receiving any funds from any institution or agency.

Declaration of competing interest

Author states no conflict of interest.

References

[1] L. De Falco, G. Savarese, T. Suero, S. Amabile, R. Ruggiero, P. Savarese, A. Fico, Detection of SRY-positive 46, XX male syndrome by the analysis of cell-free fetal DNA via non-invasive prenatal testing, Clin. Case Rep. 7 (2019) 1977−1981.

[2] V.R. Harley, M.J. Clarkson, A. Argentaro A, The molecular action and regulation of the testis-determining factors, SRY (sex-determining region on the Y chromosome) and SOX9 [SRY-related high-mobility group (HMG) box 9], Endocr. Rev. 24 (2003) 466−487.

[3] Y. Katsura, H.X. Kondo, J. Ryan, V. Harley, Y. Satta, The evolutionary process of mammalian sex determination genes focusing on marsupial SRYs, BMC Evol. Biol. 18 (2018) 3.

[4] C.L. Mitchell, V.R. Harley, Biochemical defects in eight SRY missense mutations causing XY gonadal dysgenesis, Mol. Genet. Metabol. 77 (2002) 217−225.

[5] J.L. Cunha, F.C. Soardi, R.D. Bernardi, L.E. Oliveira, C.E. Benedetti, G. Guerra-Junior, T.A. Maciel-Guerra, M.O. de Mello, The novel p.E89K mutation in the *SRY* gene inhibits DNA binding and causes the 46,XY disorder of sex development, Braz. J. Med. Biol. Res. 44 (2014) 361−365.

[6] X. Du, X. Zhang, Y. Li, Y. Han, 46,XY female sex reversal syndrome with bilateral gonadoblastoma and dysgerminoma, Exp. Ther. Med. 8 (2014) 1102−1104.

[7] M. Shahid, V.S. Dhillon, H.S. Khalil, S. Haque, S. Batra, S.A. Husain, L.H. Looijenga, A SRY-HMG box frame shift mutation inherited from a mosaic father with a mild form of testicular dysgenesis syndrome in Turner syndrome patient, BMC Med. Genet. 19 (2010) 131.

[8] Y.C. Bor, J. Swartz, A. Morrison, D. Rekosh, M. Ladomery, M.L. Hammarskjold, The Wilms' tumor 1 (*WT1*) gene (+KTS isoform) functions with a CTE to enhance translation from an unspliced RNA with a retained intron, Genes Dev. 20 (2006) 1597−1608.

[9] G.Y. Mutlu, H. Kirmizibekmez, H. Aydin, H. Çetiner, S. Moralioglu, A.C. Celayir, Pure gonadal dysgenesis (Swyer syndrome) due to microdeletion in the *SRY* gene, J. Pediatr. Endocrinol. Metab. 28 (2015) 207−210.

[10] X.B. Wang, Y.L. Liang, Z.J. Zhu, Y. Zhu, P. Li, J.P. Cao, Q.Y. Zhang, Q. Liu, Z. Li, A de novo frameshift mutation of the *SRY* gene leading to a patient with 46, XY complete gonadal dysgenesis, Asian J. Androl. 21 (2019) 522.

[11] R. Nussinov, H. Jang, C.J. Tsai, F. Cheng, Review: precision medicine and driver mutations: computational methods, functional assays and conformational principles for interpreting cancer drivers, PLoS Comput. Biol. 15 (2019), e1006658.

[12] R.C. Hunt, V.L. Simhadri, M. Iandoli, Z.E. Sauna, C. Kimchi-Sarfaty, Exposing synonymous mutations, Trends Genet. 30 (2014) 308−321.

[13] M.B.S. Al-Shuhaib, R.A. Al-Fihan, A.A. Al-Qutbi, T.M. Al-Thuwaini, Potential consequences of *DGAT2* and *BTN* genes polymorphism in Iraqi Holstein cattle, Sci. Agric. Bohem. 48 (2017) 127−141.

[14] M.B.S. Al-Shuhaib, D76V, L161R, and C117S are the most pathogenic amino acid substitutions with several dangerous consequences on leptin structure, function, and stability, Egypt, J. Med. Hum. Genet. 20 (2019) 32.

[15] V.G. Pshennikova, N.A. Barashkov, G.P. Romanov, F.M. Teryutin, A.V. Solov'ev, N.N. Gotovtsev, A.A. Nikanorova, S.S. Nakhodkin, N.N. Sazonov, I.V. Morozov, A.A. Bondar, L.U. Dzhemileva, E.K. Khusnutdinova, O.L. Posukh, S.A. Fedorova, Comparison of predictive *in silico* tools on missense variants in *GJB2, GJB6,* and *GJB3* genes associated with autosomal recessive deafness 1A (DFNB1A), Sci. World J. (2019) 5198931.

[16] B. Tang, B. Li, L.-D. Gao, N. He, X.-R. Liu, Y.-S. Long, Y. Zeng, Y.-H. Yi, T. Su, W.-P. Liao, Optimization of *in silico* tools for predicting genetic variants: individualizing for genes with molecular sub-regional stratification, Briefings Bioinf. (2019) bbz115.

[17] S.N. Hart, E.C. Polley, H. Shimelis, S. Yadav, F.J. Couch, Prediction of the functional impact of missense variants in *BRCA1* and *BRCA2* with *BRCA-ML*, NPJ Breast Canc. 6 (2020) 1−4.

[18] S.O. Conchuir, K.A. Barlow, R.A. Pache, N. Ollikainen, K. Kundert, M.J. O'Meara, C.A. Smith, T. Kortemme, A web resource for standardized benchmark datasets, metrics, and Rosetta protocols for macromolecular modeling and design, PloS One 10 (2015), e0130433.

[19] S. Wu, Y. Zhang, LOMETS: a local meta-threading-server for protein structure prediction, Nucleic Acids Res. 35 (2007) 3375−3382.

[20] M. Källberg, H. Wang, S. Wang, J. Peng, Z. Wang, H. Lu, Template-based protein structure modeling using the RaptorX web server, Nat. Protoc. 7 (2012) 1511−1522.

[21] L.A. Kelley, S. Mezulis, C.M. Yates, M.N. Wass, M.J. Sternberg, The Phyre 2 web portal for protein modeling, prediction and analysis, Nat. Protoc. 10 (2015) 845−858.

[22] Y. Wang, J. Virtanen, Z. Xue, Y. Zhang, M.R. I-Tasser, Automated molecular replacement for proteins without close homologs using iterative fragment assembly and progressive sequence truncation, Nucleic Acids Res. 45 (2017) W429−W434.

[23] A. Waterhouse, M. Bertoni, S. Bienert, G. Studer, G. Tauriello, R. Gumienny, F.T. Heer, T.A.P. de Beer, C. Rempfer, L. Bordoli, R. Lepore, T. Schwede, SWISS-MODEL: homology modelling of protein structures and complexes, Nucleic Acids Res. 46 (2018) W296−W303.

[24] R.A. Laskowski, M.W. MacArthur, J.M. Thornton, PROCHECK: validation of protein structure coordinates, in: M.G. Rossmann, E. Arnold (Eds.), International Tables of Crystallography, Vol. F, Crystallography of Biological Macromolecules, Kluwer, Dordrecht, 2001.

[25] P.C. Ng, S. Henikoff, Predicting the effects of amino acid substitutions on protein function, Annu. Rev. Genom. Hum. Genet. 22 (2006) 61−80.

[26] I.A. Adzhubei, S. Schmidt, L. Peshkin, V.E. Ramensky, A. Gerasimova, P. Bork, A.S. Kondrashov, S.R. Sunyaev, A method and server for predicting damaging missense mutations, Nat. Methods 7 (2010) 248-249.

[27] H. Tang, P.D. Thomas, Panther-Psep, Predicting disease-causing genetic variants using position-specific evolutionary preservation, Bioinformatics 32 (2016) 2230−2232.

[28] Y. Choi, G.E. Sims, S. Murphy, J.R. Miller, A.P. Chan, Predicting the functional effect of amino acid substitutions and indels, PloS One 7 (2012), e46688.

[29] E. Capriotti, R. Calabrese, R. Casadio, Predicting the insurgence of human genetic diseases associated to single point protein mutations with support vector machines and evolutionary information, Bioinformatics 22 (2006) 2729−2734.

[30] E. Capriotti, R.B. Altman, Y. Bromberg, Collective judgment predicts disease-associated single nucleotide variants, BMC Genom. 14 (2013) S2.

[31] E.M. Smigielski, K. Sirotkin, M. Ward, S.T. Sherry, dbSNP: a database of single nucleotide polymorphisms, Nucleic Acids Res. 28 (2000) 52−355.

[32] V. López-Ferrando, A. Gazzo, X. de la Cruz, M. Orozco, J.L. Gelpí, PMut: a web-based tool for the annotation of pathological variants on proteins, 2017 update, Nucleic Acids Res. 45 (2017) W222−W228.

[33] H. Carter, C. Douville, G. Yeo, P.D. Stenson, D.N. Cooper, R. Karchin, Identifying Mendelian disease genes with the variant effect scoring tool, BMC Genom. 14 (2013) 1−16.

[34] C.M. Yates, I. Filippis, L.A. Kelley, M.J. Sternberg, SuSPect: enhanced prediction of single amino acid variant (SAV) phenotype using network features, J. Mol. Biol. 426 (2014) 2692−2701.

[35] E. Capriotti, P. Fariselli, R. Casadio, I-Mutant 2.0: predicting stability changes upon mutation from the protein sequence or structure, Nucleic Acids Res. 33 (2005) W306−W310.

[36] V. Parthiban, M.M. Gromiha, D. Schomburg, CUPSAT: prediction of protein stability upon point mutations, Nucleic Acids Res. 34 (2006) W239−W242.

[37] D.E.V. Pires, D.B. Ascher, T.L. Blundell, mCSM: predicting the effects of mutations in proteins using graph-based signatures, Bioinformatics 30 (2012) 335−342.

[38] C.L. Worth, R. Preissner, T.L. Blundell, SDM-a server for predicting effects of mutations on protein stability and malfunction, Nucleic Acids Res. 39 (2012) W215−W222.

[39] D.E. Pires, D.B. Ascher, T.L. Blundell, DUET: a server for predicting effects of mutations on protein stability using an integrated computational approach, Nucleic Acids Res. 42 (2014) W314−W319.

[40] J. Cheng, A. Randall, P. Baldi, Prediction of protein stability changes for single site mutations using support vector machines, Proteins 62 (2006) 1125−1132.

[41] C.W. Chen, J. Lin, Y.W. Chu, iStable: off-the-shelf predictor integration for predicting protein stability changes, BMC Bioinf. 14 (Suppl 2) (2013) S5.

[42] C.H. Rodrigues, D.E. Pires, D.B. Ascher, DynaMut: predicting the impact of mutations on protein conformation, flexibility and stability, Nucleic Acids Res. 46 (2018) W350−W355.

[43] Y. Yang, X. Peng, P. Ying, J. Tian, J. Li, J. Ke, Y. Zhu, Y. Gong, D. Zou, N. Yang, X. Wang, S. Mei, R. Zhong, et al., AWESOME: a database of SNPs that affect protein post-translational modifications, Nucleic Acids Res. 47 (2019) D874−D880.

[44] Q. Wu, Z. Peng, Y. Zhang, J. Yang, COACH-D: Improved protein-ligand binding sites prediction with refined ligand-binding poses through molecular docking, Nucleic Acids Res. 46 (2018) W438−W442.

[45] Y. Zhang, J. Skolnick, TM-align: A protein structure alignment algorithm based on the TM-score, Nucleic Acids Res. 33 (2005) 2302−2309.

[46] C. Zhang, P.L. Freddolino, Y. Zhang, COFACTOR: improved protein function prediction by combining structure, sequence and protein-protein interaction information, Nucleic Acids Res. 45 (2017) W291−W299.

[47] M. Brylinski, J. Skolnick, A threading-based method (FINDSITE) for ligand-binding site prediction and functional annotation, Proc. Natl. Acad. Sci. U.S.A. 105 (2008) 129−134.

[48] J.A. Capra, R.A. Laskowski, J.M. Thornton, M. Singh, T.A. Funkhouser, Predicting protein ligand binding sites by combining evolutionary sequence conservation and 3D structure, PLoS Comput. Biol. 5 (2009), e1000585.

[49] H. Ashkenazy, E. Erez, E. Martz, T. Pupko, N. Ben-Ta, ConSurf 2010: Calculating evolutionary conservation in sequence and structure of proteins and nucleic acids, Nucleic Acids Res. 38 (2010) W529−W533.

[50] M.U. Johansson, V. Zoete, O. Michielin, N. Guex, Defining and searching for structural motifs using DeepView/Swiss-PdbViewer, BMC Bioinf. 13 (2012) 173.

[51] W.F. Van Gunsteren, S.R. Billeter, A.A. Eising, P.H. Hunenberger, P. Kruger, Biomolecular Simulation, The GROMOS96 Manual and User Guide, vdf Hochschulverlag AG an der ETH Zurich and, BIOMOS b.v, Zurich, Switzerland, 1996.

[52] E. Krieger, G. Vriend G, YASARA View—molecular graphics for all devices−from smartphones to workstations, Bioinformatics 30 (2014) 2981−2982.

[53] E.F. Pettersen, T.D. Goddard, C.C. Huang, G.S. Couch, D.M. Greenblatt, E.C. Meng, T.E. Ferrin, UCSF Chimera-a visualization system for exploratory research and analysis, J. Comput. Chem. 25 (2004) 1605−1612.

[54] G. Macindoe, L. Mavridis, V. Venkatraman, M.D. Devignes, D.W. Ritchie, HexServer: an FFT-based protein docking server powered by graphics processors, Nucleic Acids Res. 38 (2010) W445−W449.

[55] S. Amudha, S. Rajangam, K. Thangaraj, K. Mahalingam, SRY (sex determining regions in Y) basis of sex reversal in XY females, Int. J. Hum. Genet. 12 (2017) 99−103.

[56] N.L. Gomes, T. Chetty, A. Jorgensen, R.T. Mitchell, Disorders of sex development—novel regulators, impacts on fertility, and options for fertility preservation, Int. J. Mol. Sci. 21 (2020) 2282.

[57] C. Livermore, M. Simon, R. Reeves, I. Stévant, S. Nef, M. Pope, A.-M. Mallon, S. Wells, N. Warr, A. Greenfield, Protection against XY gonadal sex reversal by a variant region on mouse chromosome 13, Genetics 214 (2020) 467−477.

[58] V. Chandramohan, N. Nagaraju, S. Rathod, A. Kaphle, U. Muddapur, Identification of deleterious SNPs and their effects on structural level in *CHRNA3* gene, Biochem. Genet. 53 (2015) 159−168.

[59] B. Li, N.B. Phillips, A. Jancso-Radek, V. Ittah, R. Singh, D.N. Jones, E. Haas, M.A. Weiss, SRY-directed DNA bending and human sex reversal: reassessment of a clinical mutation uncovers a global coupling between the HMG box and its tail, J. Mol. Biol. 360 (2006) 310−328.

[60] C.S. Rosenfeld, Brain sexual differentiation and requirement of SRY: why or why not? Front. Neurosci. 16 (11) (2017) 632.

[61] Y. Velmurugu, P. Vivas, M. Connolly, S.V. Kuznetsov, P.A. Rice, A. Ansari, Two-step interrogation then recognition of DNA binding site by Integration Host Factor: an architectural DNA-bending protein, Nucleic Acids Res. 46 (2018) 1741−1755.

[62] R.J. Jäger, V.R. Harley, R.A. Pfeiffer, P.N. Goodfellow, G. Scherer, Familial mutation in the testis-determining gene SRY shared by both sexes, Hum. Genet. 90 (1992) 350−355.

[63] N. Nasrin, C. Buggs, X.F. Kong, J. Carnazza, M. Goebl, M. Alexander-Bridges, DNA-binding properties of the product of the testis-determining gene and a related protein, Nature 354 (1991) 317−320.

[64] V.R. Harley, D.I. Jackson, P.J. Hextall, J.R. Hawkins, G.D. Berkovitz, S. Sockanathan, R. Lovell-Badge, P.N. Goodfellow, DNA binding activity of recombinant SRY from normal males and XY females, Science 255 (1992) 453−456.

[65] E.M. Maier, C. Leitner, U. Löhrs, U. Kuhnle, True hermaphroditism in an XY individual due to a familial point mutation of the *SRY* gene, J. Pediatr. Endocrinol. Metab. 16 (2003) 575−580.

[66] A. Tajouri, D. Ben Gaied, S. Hizem, S. Boujelben, F. Maazoul, R. M'rad, F. Poulat, M. Kharrat, Functional Analysis of Mutations at Codon 127 of the *SRY* gene associated with 46,XY complete gonadal dysgenesis, Sex Dev. 11 (2017) 203−209.